Resources, Environment and Sustainability 5 (2021) 100031

Contents lists available at ScienceDirect

Resources, Environment and Sustainability

journal homepage: www.elsevier.com/locate/resenv

Probability of glacial lake outburst flooding in the Himalaya

Litan Mohanty, Sabyasachi Maiti *

Department of Geology and Geophysics, Indian Institute of Technology Kharagpur, India

ARTICLE INFO

Keywords:
Glacial lake
Himalaya
Object-based classification
AHP
GLOF

ABSTRACT

The present study aims to determine the probability of glacial lake outburst flooding (GLOF) in the Himalaya. Here, a total of 4198 glacial lakes with larger dimensions (>0.01 km^2) were considered. A fusion between Object-based classification (OBC) and Analytical Hierarchy Process (AHP) was applied for unbiased results, involving the fifteen most essential predictors. The previously studied threshold values of predictors were used in OBC to determine GLOF prone lakes. On the other hand, earthquake, lake freeboard, moraine dam steepness, avalanches, and lake size change rate were prioritized for the AHP method. Individually, OBC and AHP methods identified 107 and 224 critical lakes. However, as a fusion of the above techniques (GIS overlay analysis), our study identified 60 critical lakes, followed by 164 and 3974 glacial lakes with medium and lower probability of GLOF. 95% of the higher GLOF-probable lakes are concentrated in the Kosi (33), Pelkhu (7), and Tista (5) river basins; sub-regionally coincide with Sikkim, Everest, Bhutan and Langtang region.

1. Introduction

The global mean temperature has been increasing at a higher rate since 1980 (Mayewski and Jeschke, 1979; Richardson and Reynolds, 2000; Kulkarni et al., 2007, 2011). As a result, glaciers are melting at an alarming rate forming glacial lakes (Mool et al., 2001; Bajracharya et al., 2008a,b; Kääb et al., 2012; Gardelle et al., 2013; Bolch et al., 2012; Mohanty and Maiti, 2021). The melting of ice can produce liquid water and remove the support system for the upper ice or soil layer (Joughin et al., 2014; Kääb et al., 2018). The meltwater can lead to the destabilization of cryospheric environments, including glacier collapse (Deline et al., 2015; Falaschi et al., 2019), rock and ice avalanche (Chiarle et al., 2007; Dufresne et al., 2019), glacier and snow melting flood (Brown et al., 2014; Duan et al., 2020), ice shelf decay (Feldmann and Levermann, 2015; Hogg and Gudmundsson, 2017), glacial lake outburst flood (GLOF) (Bajracharya and Mool, 2009; Harrison et al., 2018; Veh et al., 2019), and thermokarst development (Nelson et al., 2002; Saito et al., 2018). All above cryospheric hazards are concentrated within lands (Ding et al., 2020). Amongst these, GLOF is very devastating, as it can travel to the longest distance up to 200 km with a peak discharge of 30,000 m^3/s and a speed of 14 to 18 km/h (Sattar et al., 2019, 2020; Ding et al., 2020; Richardson and Reynolds, 2000).

GLOF is a phenomenon of massive amounts of water flowing in a narrow river channel originating from natural dam failure (Clague and Evans, 2000; Huggel et al., 2002; Huggel, 2004). GLOF events have widely been reported around the world's high mountains, like Himalayas, Andes, and Rockies (Nie et al., 2018; Worni et al., 2013; Emmer et al., 2016; Allen et al., 2016). However, amongst all types of natural disasters occurring globally, the maximum numbers of GLOFs have been reported in Central Asia (Alcántara-Ayala, 2002; Carrivick and Tweed, 2016). Other sources (Veh et al., 2020) said a total of 39 GLOFs in the Himalayas. The recent GLOF occurred in Chamoli district on Feb 7, 2021, followed by Chorabari lake outburst in Kedarnath in July 2013. Both claimed a thousand lives and a million-dollar loss of properties (Das et al., 2015; Meena et al., 2021). Gongbatongshaco in 2016 (Cook et al., 2018) and Jinwuco in 2020 (Zheng et al., 2021) are other few examples, alongwith many unnoticed GLOFs (Nie et al., 2018). GLOF events mainly occurred for ice-dammed lakes and a few moraine dam lakes (Carrivick and Tweed, 2016). However, the number of moraine-dammed lakes induced flooding were globally reducing since the mid-1990s.

Many researchers (Aggarwal et al., 2017; Huggel, 2004; McKillop and Clague, 2007; Mool et al., 2001) have mapped critical lakes linking broadly four elements: lake (change rate, lake dimensions), moraine dam (type, steepness, width to height ratio, ice core, etc.), mother glacier (proximal distance, calving width, frontal steepness, etc.) and geomorphology/ triggering parameters avalanches, earthquake) (Table 1). However, integration of these parameters involves techniques like remote sensing (Huggel et al., 2002; Kääb and Reichmuth, 2005; Fujita et al., 2009), hazard scoring (ICIMOD, 2001), geographic information systems (GIS) (Huggel et al., 2002; Huggel, 2004), overlay analysis (Zaidi et al., 2013), AHP (Aggarwal et al., 2017), statistical (McKillop and Clague, 2007), empirical (Huggel, 2004; McKillop and Clague, 2007) methods, and fusion of vulnerability-cum exposure indices (Allen et al., 2016; Wilson et al., 2015; Zheng et al., 2021).

* Corresponding author.
E-mail address: maiti@gg.iitkgp.ac.in (S. Maiti).

https://doi.org/10.1016/j.resenv.2021.100031
Received 13 April 2021; Received in revised form 17 July 2021; Accepted 17 July 2021
Available online 28 July 2021

Table 1
List of parameters for GLOF susceptibility mapping.

Triggering factor	Lake characteristic	Dam characteristic	Glacial/basin characteristic
Landslide	Lake area	The width of the crest of the moraine	Glacier retreat rate
Avalanches	Lake volume	Dam flank steepness	Watershed
Earthquake	Unstable lake upstream	Lake freeboard to moraine crest height ratio	The slope of accumulation area of mother glacier
	Elevation of lake	Lake freeboard	The slope of the glacier tongue
	Length of lake	Ice-cored moraine	The distance between glacier and lake
	Width of lake	Main rock type of moraine	Crevassed glacier snout
	Orientation of lake	Moraine vegetation coverage	The slope between the lake and Glacier snout
	Lake type	Moraine height to width ratio	Lake glacier relief
	Change rate	Moraine height	Geomorphology
	Drainage type of the lake	Moraine height to area ratio	Distance of settlement
	The activity of the lake		Glacier size
	Glacier-fed lake		Glacier calving frontal width

Besides, deterministic methods of GLOF modelling (Washakh et al. 2019; Sattar et al., 2019; Sattar et al., 2021; Goswami and Goyal, 2021) and lake size change analysis (Worni et al., 2013; Nie et al., 2017; Nie et al., 2019) were adopted for critical lakes detection with an estimation of their local flood root and peak discharge. However, regional GLOF probability assessment is relatively lacking in the Himalaya. At the same time, the results of different studies are often uncomparable because of differences in lake inventories, indicator selection and classification methods. Thus, we here tried to identify lakes with potentially high GLOF risk by combining OBC and AHP methods on a regional scale. The Analytic Hierarchy Processes (AHP) method was used in various natural hazard studies (see Section 3.7) (Ayalew et al., 2005; Lari et al., 2009; Iribarren Anacona et al., 2014; Wang et al., 2016) that allows evaluating the consistency (Saaty, 1987) of the judgements, based on the estimation of the eigenvalues of the factors matrix. Besides, the object-based classification (OBC) techniques use the threshold values of different controlling parameters to identify critical lakes (MacLean and Congalton, 2012). Here, we used the maximum number of predictor variables involving remote sensing and GIS techniques to detect the GLOF prone lakes in the Himalaya.

2. Study area

Glacial lakes are densely distributed throughout the Himalaya (Gardelle et al., 2011; Zhang et al., 2015; Nie et al., 2017). Eastern Himalayan glacial lakes are expanding and increasing at an alarming rate than western and central Himalaya (Gardelle et al., 2011; Zhang et al., 2015; Nie et al., 2017). For developing countries like India, Nepal and Bhutan, GLOF is a severe threat (Alcántara-Ayala, 2002; Carrivick and Tweed, 2016). Therefore, the predetermination of GLOF prone lakes plays an essential role in environmental safety and management.

Here we have chosen Himalayan region with an approximate linear extent of 2400 km from northwest to southeast, bounded between 69° 48' 36.73'' to 98° 22' 22.78''E longitude and 27° 12' 16.89'' to 39° 31' 26.89''N latitude (Fig. 1). The entire Himalaya varies in width from 400 km west to 150 km east with 5390 m average elevation and spreads across five countries like Nepal, India, Bhutan, China, and Pakistan. It contains ~22,800 km^2 glaciers area with 1071 km^3 approximate snow volume (Farinotti et al., 2019; Bolch et al., 2012). The distribution of glaciers and equilibrium line altitudes is mainly due to three types of wind flows such as (i) NW wind flow (westerly), (ii) SW Indian monsoon, and (iii) NE wind flow (Yao et al., 2012; Bolch et al., 2012; Bookhagen and Burbank, 2010). The Eastern Himalaya got snow by SW Indian monsoon and NE wind flow, mainly during summer time. This zone is a summer accumulation type glacier. Other western side of the Himalaya (i.e., Karakoram, Pamir and west Himalaya) is getting snow by westerly during wintertime; hence, it is called winter accumulation type glaciers. Monsoonal precipitation decreases from east to west, and the western extremity of the monsoonal precipitation zone is present at 78° longitudes near Sutlej valley (Bookhagen and Burbank, 2010). The northern side of eastern Himalaya gets fewer snowfalls than the southern side by monsoonal precipitation due to the shadow effect (Bookhagen and Burbank, 2010). The spatial distribution of precipitation showed that the precipitation amount decreases from east to west along the Himalayan arc (Bookhagen and Burbank, 2010).

3. Methodology

3.1. Data source

3.1.1. Satellite data and DEM

Landsat thematic mapper (TM) and operational land imager (OLI) were downloaded from the Earth Explorer (USGS) webpage. A total of 75 Landsat scenes were used in this study. Moreover, ALOS-PALSAR DEM was used in this study for various purposes. Satellite data with cloud cover <5% were selected using Earth Explorer's filters. Since we are working on glacial lake monitoring, chosen months coincide with new snow melting seasons (Gardelle et al., 2011). Thus, satellite images were selected from September to November for the eastern Himalaya; and from June to October for the western, avoiding consequences of high cloud and snow coverage.

3.1.2. Lake data

Initial lake boundaries were collected for 1990, 2000 and 2010 from the inventory of Zhang et al. (2015). A few new lake boundaries and corrections of existing ones (e.g., shadow) were carried out. Besides, for 2015 and 2019, we used Landsat OLI and high-resolution images (Worldview, Quickbird and GeoEye) for updating our lake inventory.

3.2. Glacial attribute derivation

3.2.1. Glacier boundary delineation

Glacier sizes were estimated from the glacier boundary RGI 5.0 version. However, the data was not used exclusively because its outlines did not match the observed glacier extents; hence, some corrections were done on this data based on the satellite images in false colour composite (FCC) (Kargel et al., 2005).

3.2.2. Ablation area delineation

Ablation areas were demarcated using ALOS-PALSAR DEM and glacier boundary shapefile following the clue that a glacier's median elevation is the equilibrium line altitude (ELA) (Racoviteanu et al., 2014), i.e., the boundary between an accumulation area and ablation area. The distinction of the ablation area was performed using ArcGIS 10.3.

3.3. Lake attributes derivation

3.3.1. Lake characteristic

Different types of lakes (glacier-fed, connected, moraine-dammed lake) were marked in the attribute table of glacial lake polygon by visual inspection in Google Earth and Landsat images. Some parameters were taken from Zhang et al. (2015). Proximal distances were calculated by the near distance tool. While calculating, lake and glacier

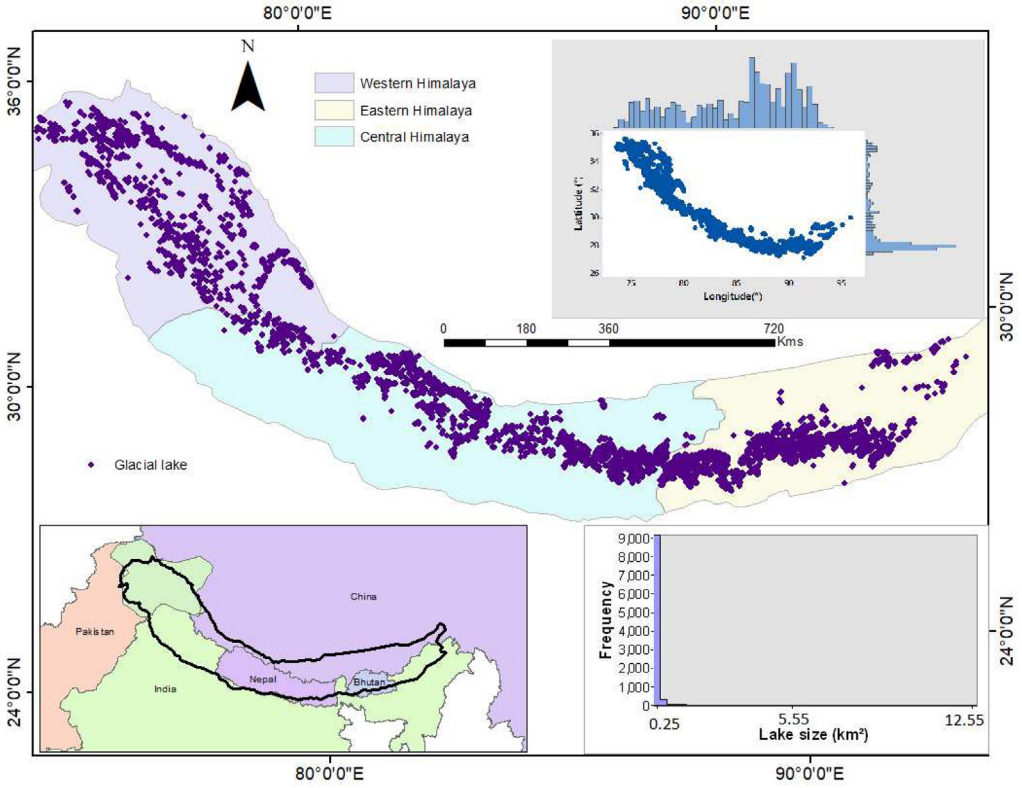

Fig. 1. Study area map with three subdivisions of eastern, central and western Himalaya. The lake locations are shown in violet dots. The distribution of lakes along latitude and longitude is shown in the histogram. Lake size distribution is also shown in the histogram.

polygon were utilized as an input file. Additionally, lake length and width were calculated by using minimum boundary geometry in ArcGIS 10.3. Crevassed glacier, glacier calving frontal width, snout steepness were marked in Google Earth platform and calculated in ArcGIS 10.3 software. Lake depth and volume were calculated from the empirical formula reported by Huggel et al. (2002). Dam area, dam steepness, height and lake freeboard were demarcated using the ALOS-PALSAR digital elevation model (DEM). The characteristics of mother glaciers (slope of an accumulation area, size of the glacier, debris content) were extracted using ENVI 5.3 and joined to the lake attribute in the ArcGIS platform (Racoviteanu et al., 2014). All the derived lake attributes were listed in Table 1.

3.3.2. Lake size change rate

The average lake size change rate was estimated due to inconsistency in their appearance (i.e., some have formed after 2000, whereas few were absent after 2015). The average lake size change rate was calculated using suitable lake pairs with 10 years intervals (e.g., 1990 to 2000, 2000 to 2010, 2015 to 2019 etc.) given in Eq. (1).

$$\text{Average lake size change rate } (m^2/\text{year}) = \frac{\sum_1^n X_i - X_{i-10}}{m * n} \quad (1)$$

Where X_i and X_{i-10} are the lake size with 10 years interval, m is the total period of study, and n is the number of lake size change studies in a specific interval (here 10 years).

The standard deviation of all individual lake size change rates was used as an error. This value might be higher than the average value of lake size change rate as most of the lake shows a higher -ve lake size change rate due to GLOF where some lake showed a higher increase in lake size.

3.4. Controlling parameter generation

3.4.1. Avalanches

Ice avalanches are the most common cause of outbursts of floods in the Himalaya (Wang et al., 2011) and tropical Andes (Lliboutry et al., 1977). Ice avalanches usually occur in temperate glaciers with a steep slope (≥25°) (Alean, 1985). These can generate impulse waves within lakes and cause dam overtopping. An ice avalanche's likelihood of influencing a lake depends on the distance, slope, and roughness of the terrain between glacier and water bodies. We used AHP methods for estimating avalanche probability maps using parameters like relief, slope, curvature, ground cover and aspect with weights (0.28, 0.31, 0.09, 0.18 and 0.14) (Kumar et al., 2017; Marana, 2017).

3.4.2. Landslide

Steep non-vegetated slopes are a common source of mass movements (Peduzzi, 2010) and indicate high geomorphic activity. Massive and high-velocity landslides can generate large waves in the lake water, which can suddenly drain lakes with or without breaching a dam (Clague and Evans, 2000; Walder et al., 2003). Such mass induced outburst floods were seen in Patagonia and other Andean regions (Hubbard et al., 2005; Harrison et al., 2006) with peak ground acceleration (PGA) was >0.6 g and slope >30° (Kargel et al., 2016). Here, we used the landslide probability data of Hartmann and Moosdorf (2012); these authors have derived the landslide probability map for the Earth's total land surface. A buffer of 500 m was taken around the lake, and the average values were assigned in ArcGIS 10.3 software.

3.4.3. Earthquake

Earthquake occurrence data was downloaded from the USGS webpage. A total of 39 (1980–2019) years of data was taken during our derivation of earthquake occurrences density map. While making the density map, the output cell size of 500 m was given, a window size of 5 × 5 was assigned in ArcGIS 10.3. Earthquake occurrences higher

than 4 magnitudes were chosen, in accordance with previous claims by Keefer (1984, 2002) that earthquake M > 4 could generate landslides and other mass movements. Thus a total of 1509 earthquake locations were considered all along Himalaya.

3.5. Climatic data

Precipitation data, i.e., TRMM (Tropical Rainfall Measuring Mission) and skin temperature data, were taken from the Giovanni webpage. TRMM was launched from the GODDARD space application centre by USGS's collaborated work (United States Geological Survey) and JAXA (Japan Aerospace Exploration Agency). For the regional temperature and precipitation study, a spatial resolution of 0.25° × 0.25° gridded data was taken for the whole Himalaya from 1984–2020 (Kanamitsu et al., 2002; Bookhagen and Burbank, 2010).

3.6. Controlling parameters

Hazard can be defined as the probability of occurrences and an event's magnitude (Huggel, 2004). Here, we used various parameters for GLOF prediction and estimating flood water volume. Thus, we estimate both the probability and magnitude of GLOF. Previous studies indicated that the possibility of a GLOF is a function of several variables. Earlier researchers (Chen et al., 1999; Lu et al., 1999; Bajracharya et al., 2008a,b) have suggested seven variables based on previously drained glacial lakes on the Tibetan Plateau. On the other hand, McKillop and Clague (2007) have listed 18 potential predictor variables based on previously documented incidents of moraine dam failures. However, some of their proposed variables can only be detected from high-resolution satellite images or field observation. However, it is practically impossible for a regional glacial lake evaluation by fieldwork due to remoteness and harsh weather conditions. In the present study, 15 parameters were uniformly used all along the study area. Considering lake characteristics, lake-glacier relationship, dam characteristics, and glacial or basin characteristics, we infer here probability of GLOF in the future (Table 1). Dam characteristics like lake freeboard, dam steepness and dam height play a significant role for GLOF. Subsequently, lake size and lake size change rate are the most effective GLOF probability mapping parameters (Worni et al., 2013; Aggarwal et al., 2017; Nie et al., 2017). Moraine dammed lakes are more prone to GLOF as reported by various authors, and connected lakes have a higher change rate than unconnected lakes (Chen et al., 1999; Lu et al., 1999; Bajracharya et al., 2008a,b; McKillop and Clague, 2007). Glacier and lake-related parameters also have a crucial role in determining GLOF; thus, glacier-fed lake, proximal distance, glacier snout steepness, glacier calving frontal width was used for GLOF probability determination (Huggel et al., 2002; ICIMOD, 2011). Lakes in contact with glaciers can be affected by calving and the sudden floating of dead ice. Both mechanisms can produce waves capable of dam overtopping, breaching and subsequent dam failure (Richardson and Reynolds, 2000). Glacier fed lakes and lakes with lesser proximal distance (<500 m) are prone to lake expansion, thus dangerous depending on local geomorphology. Lake dimensions have been directly related to outburst volume, peak discharge and the flood damage potential (Costa and Schuster, 1988). However, a lake of size (>0.01 km^2), volume (>0.01 km^3), width (>0.01 km) and length (0.01 km) is prone to GLOF (Li et al., 2021; ICIMOD, 2011; Worni et al., 2013). Similarly, elevated lakes with a higher force of gravity (viz. >3500 m) are also susceptible to GLOF (Lu et al., 1999; Huggel et al., 2002; ICIMOD, 2011). A glacier with a low-angle terminus can be an indicator of a negative mass balance.

Consequently, lakes in contact with flat glacier fronts (slopes less than 5°) are likely to grow due to glacier retreats (Frey et al., 2010). Steep outlets can be more easily enlarged than low-gradient outlets if an increase in lake discharge occurs. Progressive erosion can widen and deepen the outlet leading to lake drainage. Consequently, dams with steep outlets are more susceptible to failure (O'Connor et al., 2001).

Landslides and avalanches are closely spaced to the epicentre of an earthquake (Keefer, 2002, 1984). Earthquakes can directly affect the glacial lake or indirectly by creating landslides and avalanches (Kargel et al., 2016; Zhao et al., 2018). Influencing parameters like earthquakes, avalanches, and landslides control GLOF for all types of glaciers (Huggel et al., 2002; ICIMOD, 2011). Steep unvegetated slopes are a common source of mass movements (Peduzzi, 2010) and can be indicators of high geomorphic activity. These influencing parameters can form GLOF in all types of lakes. GLOFs caused by the collapse and erosion of moraine dams rarely result in total lake volume drainage. The expanding rate of glacial lakes (lake size change rate> 1000 m^2/yr) is one of the most important indicators of potential outburst hazards (Wang et al., 2012; Worni et al., 2013; Nie et al., 2017). Lake type also indirectly denotes the change rate of lake size, thus being crucial for GLOF mapping as input parameters. Glacial lake size and potential flood volumes directly control a hazard's severity (Fujita et al., 2013; Worni et al., 2013). Meanwhile, monitoring glacial lake changes at regional scales, especially considering the Himalaya as a whole, is essential to assessing climate change impacts (Nie et al., 2017). Lake size is directly related to the flood volume, lake length, lake width, and water volume (Huggel et al., 2002).

3.7. Object-based classification method

Object-oriented image classification involves identifying image objects, or segments, that are spatially connecting pixels of similar texture, colour and tone (MacLean and Congalton, 2012). Relationships between objects can play an essential role in their identification and classification. Object-based classifiers classify not a single pixel but groups of pixels representing existing objects in a GIS database. This approach is based on a supervised maximum likelihood classification. To avoid the problem of defining data-dependent thresholds, we applied an object-based supervised classification approach. Here, the same idea was used for identifying the GLOF prone lakes from the different parameters of the lakes and their surrounding areas. The threshold value for GLOF determination was taken, as defined by various researchers (Lu et al., 1999; Huggel et al., 2002; ICIMOD, 2011).

The OBC method was used for the GLOF probability determination. A threshold value is always required for getting the subsequent output in a chain of the object-based classification method. Thus, the parameters whose threshold has already been determined for deciding GLOF occurrences were taken. A total of 15 parameters such as lake size change rate, lake size, lake freeboard, dam steepness, lake elevation, glacier snout steepness, lake length, lake freeboard, moraine-dammed lake, glacier-fed lake and proximal distance, and some influencing parameters: earthquake, avalanches and landslides were considered for the study (Fig. 2). A series of queries in ArcGIS10.3 software was subsequently used to demarcate GLOF prone lakes in the Himalaya. Thresholds of the probable GLOF denoting parameters were taken from various works done previously (Aggarwal et al., 2017; Huggel et al., 2002; Iribarren Anacona et al., 2014; ICIMOD, 2011; Lu et al., 1999). All the influencing parameters and glacial and lake parameters were used simultaneously, or dam parameters were considered for demarcating GLOF prone lakes. Earthquake density >1, avalanches >5 and landslide >5 were taken for identifying GLOF-prone lakes in the OBC technique (Fig. 2).

3.8. AHP method

Analytical Hierarchy Process (AHP) (Saaty, 1987) formulates and assists in decision making by assigning ranks and weights to the attributes using matrix operation. It uses hierarchical structures to quantify relative priorities for a given set of elements on a ratio scale. The judgements between two particular parameters can be done by a

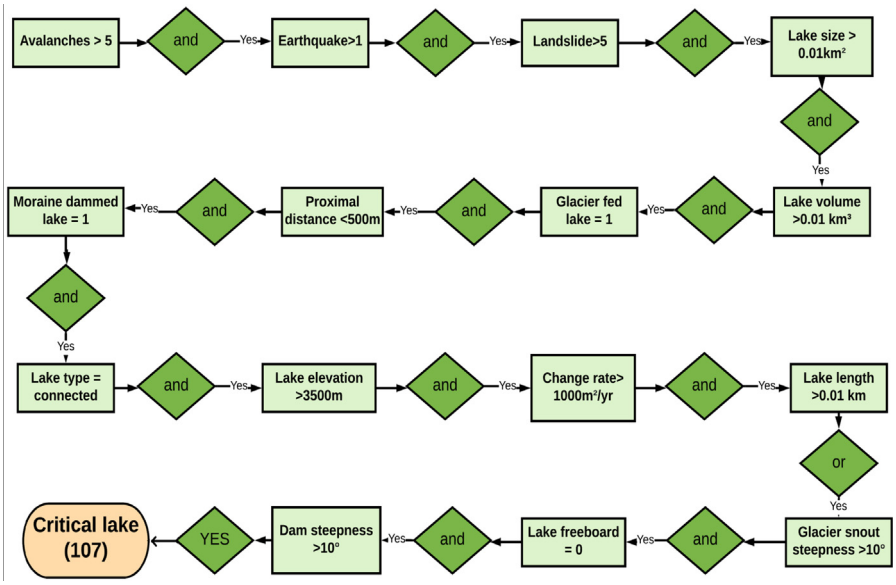

Fig. 2. The object-based classification method flow diagram.

pairwise comparison on a 1–10 scale, and a pairwise comparison matrix is constructed from that comparison. In this 1–10 scale, the values 1, 3, 5, 7, and 9 indicate that the two elements are either 'equal' or 'slightly' or 'strongly' important than others. The pairwise comparison matrix was used to derive the individual normalized weights of each element by computing the principal eigenvector. The results in a matrix range from 0 to 1 and add up to 1 in each column. The weights of each criterion are calculated by averaging the values of each row of the matrix.

Each thematic map feature is also normalized between 0 and 10 (Nath, 2004) to ensure that no layer exerts influence beyond its determined weight. Normalization is carried out for the features using the relation:

$$X_i = \frac{R_j - R_{min}}{R_{max} - R_{min}}$$

R_j is the raw rating, R_{max}, and R_{min} are the maximum and minimum ratings of a particular layer.

The consistency ratio (CR) in the AHP method shows the probability that the decision matrix was randomly created.

$$CR = \frac{CI}{RI}$$

Where RI average of the resulting consistency index, depending on the order of the matrix, given by the Saaty, and CI is the consistency index and can be expressed as

$$CI = \frac{(\lambda_{max} - n)}{(n-1)}$$

The largest or principal Eigenvalue of the matrix can be easily calculated from the matrix, and n is the matrix's order. If the CR value is more significant than 0.1, the AHP can be rejected. The acquisition weights were employed by using a weighted linear sum procedure. Furthermore, the acquisition weights were employed to calculate the GLOF probability model.

Each layer's weightage was calculated from a spreadsheet package called expert choice from AHP (Nath, 2004; Aggarwal et al., 2017). It calculates the weightage of each parameter from multiple criteria decisions with the pairwise comparison. These weight calculations are done outside the GIS platform and then applied in the raster calculator tool in ArcGIS 10.3 software. Fifteen thematic layers were used for this study, and the respective weights assigned to the layers were described in Table 2. Consistency ratio (CR) and principal Eigenvalue were estimated as 9.7% and 17.147, respectively, from the decision matrix.

Table 2
Weightage of input parameters for GLOF probability mapping derived from AHP calculator.

Thematic layers	Weight
Proximal distance	0.047
Glacier calving frontal width	0.052
Glacier snout steepness	0.055
Lake type	0.057
Lake area change rate	0.071
Lake volume	0.026
Lake size	0.056
Lake elevation	0.02
Lake aspect	0.018
Avalanches	0.081
Landslide	0.051
Earthquake	0.167
Dam steepness	0.106
Lake freeboard	0.161
Dam height	0.032

In this method, lake polygons were converted to raster with 30 m spatial resolution. The continuous parameters were reclassified into ten classes by quantile classifier, and the categorical variables were also reclassified. Weights were assigned to each of the classes by expert knowledge. The quantile classifier used in this study divides classes so that the total numbers of features in each category are approximately the same.

3.9. Merging procedure of OBC and AHP results

Both AHP and OBC methods show different critical lakes due to their variable dependency: one on the data distribution and others on the expert's choice. However, their combined result provides an effective GLOF probability. We merged both using overlay analysis; the higher probable lake derived from AHP (>8) and object-based classification method, and the common one is taken as the higher GLOF-potential lake (Fig. 3). Furthermore, the rest of the higher probable lakes from these two methods are the second most probable lakes. The remaining number of lower GLOF-probable lakes were categorized as the lowest probability.

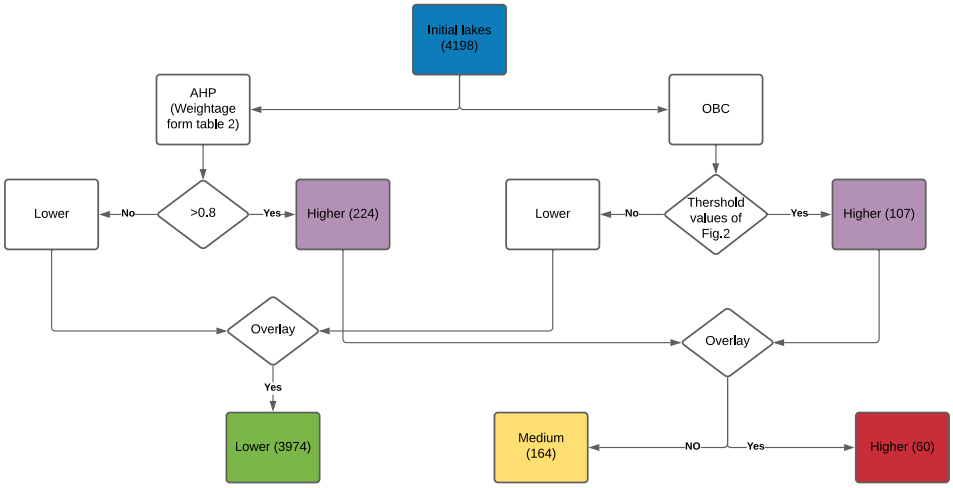

Fig. 3. Flow diagram for merging procedures of two output results generated from AHP and OBC method.

4. Result

4.1. GLOF probability estimation by OBC method

Total 107 out of 4198 glacial lakes were identified as GLOF-prone. The supraglacial lakes and glacial lakes size >0.01 km^2 were eliminated from our GLOF probability analysis. Thresholds were used as discussed in the methodology part to get the result. These higher GLOF prone lakes were gathered in eastern, central and western Himalaya, respectively. Thorthormi, Imja, Lhonak, Gangxico, Pinda, Longbasa lakes got higher GLOF probability in the OBC method. Larger lakes with high expansion rates have been already reported as supercritical lakes (Bolch et al., 2008; Mool et al., 2008; Nie et al., 2012; Worni et al., 2013).

4.2. GLOF probability estimation by AHP method

A total of 224 lakes were identified as high GLOF-prone in the AHP result. In the hierarchical analytical process, 15 thematic layers, viz., earthquake, lake freeboard, dam steepness, avalanches, lake size change rate and lake type, got higher weightage. Aggarwal et al. (2017) gave a similar weightage for GLOF probability mapping. Besides, lake aspect, lake elevation, lake volume, dam height, proximal distance, and landslide gave the lowest weightage to GLOF. Most of the lakes were gathered in eastern Himalaya followed by central and western.

4.3. Merging of OBC and AHP results

A total of 60, 164 and 3974 glacial lakes are coming under a higher, medium and lower probability of glacial lake outbursts in the Himalaya out of 4198 lakes (>0.01 km^2). Most glacial lakes showed a concentration over the eastern Himalaya, followed by central Himalaya and western Himalaya. Besides, various researchers have classified Himalayan into sub-regions like Sikkim, Nepal, Bhutan, Langtang, Everest Himalaya and Uttarakhand. Lakes with higher susceptibility to GLOF were clustered in Bhutan, Everest, Sikkim, and Langtang regions (Fig. 4). Moreover, basin wise distribution of Himalayan glaciers showed that these are clustered primarily on Manas (846), Kosi (707), upper Indus (675), Yarlung Zangbo (385) and Karnali (354). However, most of the higher probable lakes are concentrated in the Kosi (33), Pelkhu (7), Tista (5) and Karnali (3) (Table 3).

5. Discussion

5.1. Overcoming of AHP's limitations

AHP is a simple, versatile, user-friendly and frequently used method in GIS integration in almost all fields: landslide susceptibility mapping (Kayastha et al., 2013), urban planning (Bathrellos et al., 2012), mineral exploration (Hosseinali and Alesheikh, 2008), GLOF probability (Aggarwal et al., 2017), avalanches probability (Kumar et al., 2017). In this part, conditioning and triggering factors were weighted using a pairwise comparison matrix. The subdivisions of each class were weighted manually to get the corresponding rating and measuring consistency ratio. This method has some limitations: a 9-point predefined scale, making it hard to decide on time limitation and subjective evaluation. Moreover, another constraint is that the AHP method needs a manual weighting scheme. However, this venture represents a practical approach in data-sparse regions such as Sikkim (Aggarwal et al., 2017). To overcome this problem and for the betterment of our result, we used the object-based method. Combining these two results gives a better and unbiased result.

5.2. Glacier retreat related to lake number and size change in the Himalaya

Glaciers in the Himalaya are retreating faster; thus, glacial lakes also increase in size and number in the study area (Nie et al., 2016; Worni et al., 2013). There were exceptions like Karakoram, where glaciers are gaining mass with a decrease in lake size by surging, thus forming occasional GLOF (Kulkarni et al., 2007; Gardelle et al., 2011; Bolch et al., 2012; Kääb et al., 2012; Brun et al., 2019). Other than this, all regions show lake size increase at a different rate (Aggarwal et al., 2017; Komori, 2008). The glacial lake number was estimated as 2471, 2518, 2994, 3556 and 4081 in 1990, 2000, 2010, 2015 and 2019. Lake size also showed an increasing trend since 1990, with an average lake size change rate of 400.85 ± 1146.63 m^2/yr. Here, the higher standard deviation is due to high variation in lake size due to GLOF. In the Himalaya, 3386 glacial lakes are increasing in size out of 4198 lakes, and these are mostly moraine dams, glacier-fed, and larger-sized lakes (>0.01 km^2). Glacier-fed lakes get water from direct precipitation and primarily from glacier meltwater; therefore, these lakes have a higher expansion rate. Those can be dangerous depending on other parameters (local geomorphology). Zhang et al. (2015) have also shown those glaciers fed lakes are increasing in size at a higher rate than the non-glacier fed lakes. Moreover, some glacial lakes in western and Arunachal Himalaya showed a decreasing trend, whereas central and eastern Himalayan lakes showed an increasing trend at a higher rate (Gardelle et al., 2011). These decreases in lake size are mostly for non-glacier fed, unconnected and erosional lakes.

Table 3
Higher GLOF prone lake and lake distribution along the river basin and sub-basin of the Himalayas.

Broad division	Main basin	Sub-basin	Total glacial lakes	High GLOF prone lakes			% of high GLOF prone lakes with respect to total glacial lakes			% of high GLOF prone lakes w.r.t total high GLOF prone lakes
				Main basin wise	Sub-basin wise	Broad division	Main basin wise	Sub-basin wise	Broad division	
Western	Indus	Panjnad	301	4	3	4	0.4	0.99	0.4	6.66
		Upper Indus	675		1			0.14		
Central	Ganga	Pelkhu	18	46	7	38	3.71	38.88	3.06	76.66
		Yamuna	5		0			0		
		Upper Ganga	27		0			0		
		Karnali	354		3			0.84		
		Gandaki	127		3			2.36		
		Koshi	707		33			4.66		
Eastern	Brahmaputra	Punatsang Chu	333	10	1	18	0.52	0.3	0.94	16.66
		Yarlung Zangbo	385		1			0.25		
		Kameng	56		0			0		
		Manas	846		3			0.35		
		Amo Chu	78		1			1.28		
		Tista	165		5			3.03		
		Subansiri	39		0			0		

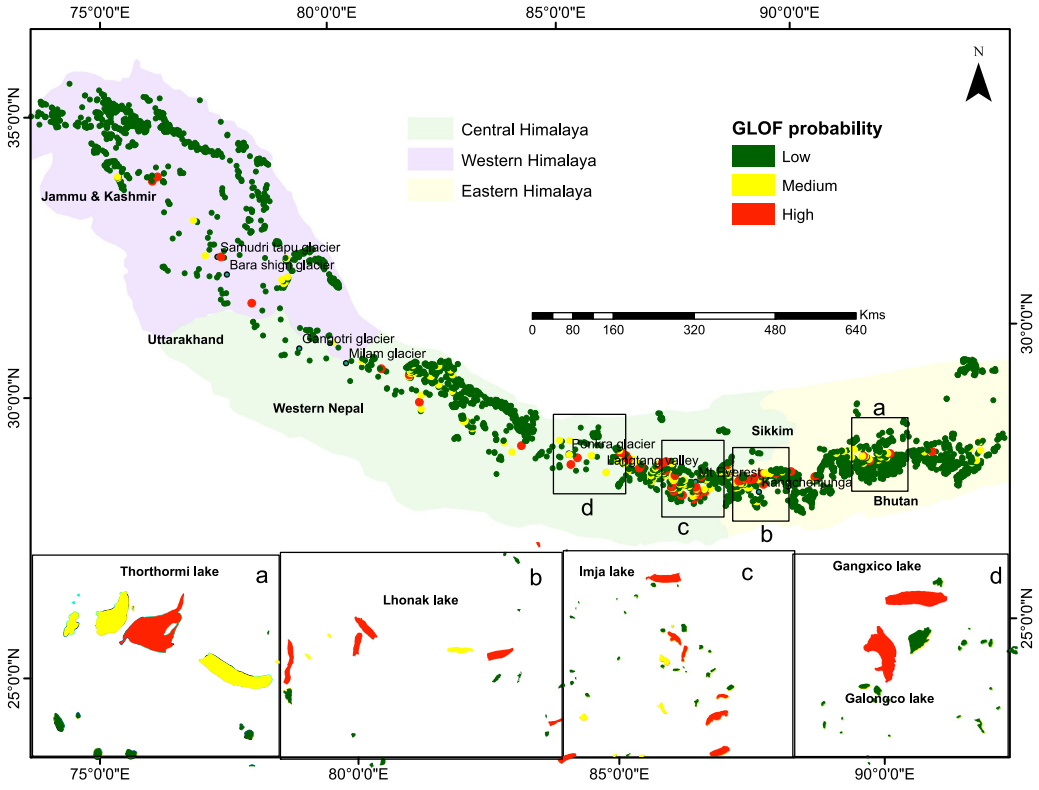

Fig. 4. GLOF probability lake distribution in the Himalayas; here with zoom boxes a to d some important lakes were shown. Here, red, yellow, and green indicate the higher, medium, and lower GLOF prone lakes. Lake counts of individual categories are shown in the histogram.

5.3. Climatic control on GLOF

Opposite precipitation trends (from 1998 to 2020) were observed between the eastern and western Himalaya (Fig. 5). Precipitation is rising in the western part; an opposite trend was noticed in the eastern and central Himalaya. This precipitation fall caused the glaciers to retreat faster; thus, the lake expansion rate is higher in the east and central Himalaya. Additionally, the glacial skin temperature record (from 1981 to 2020) showed a rising trend; essentially may control future lake formation and growth. Various locations of Himalaya (Gardelle et al., 2011; Nie et al., 2017), viz, Boshula mountain (Wang et al., 2011), Uttarakhand (Bhambri et al., 2011), Sikkim (Racoviteanu et al., 2014); Everest (Bolch et al., 2012); Jammu and Kashmir (Ghosh et al., 2014); Bhutan (Bajracharya et al., 2014) reported same. The warming and precipitation reduction are accelerating the frequency of avalanches; and triggering more GLOFs (Liu et al., 2014; Carrivick and Tweed, 2016). In the central to eastern Himalaya, there is a higher chance for lake volume increase seeing the nature of temperature and precipitation pattern and their trend.

5.4. Google earth and field validation

All higher GLOF probable lakes exhibit lesser lake freeboard, larger size, dammed by moraine and higher lake expansion rate. Google earth image was used for detailed mapping and verification. In Fig. 6, we choose lakes (A to J) to understand GLOF probability clearly. Lakes B and D are found as giant lakes and located upstream of A and C, respectively. Similarly, lake J is situated downstream of three lakes, G,

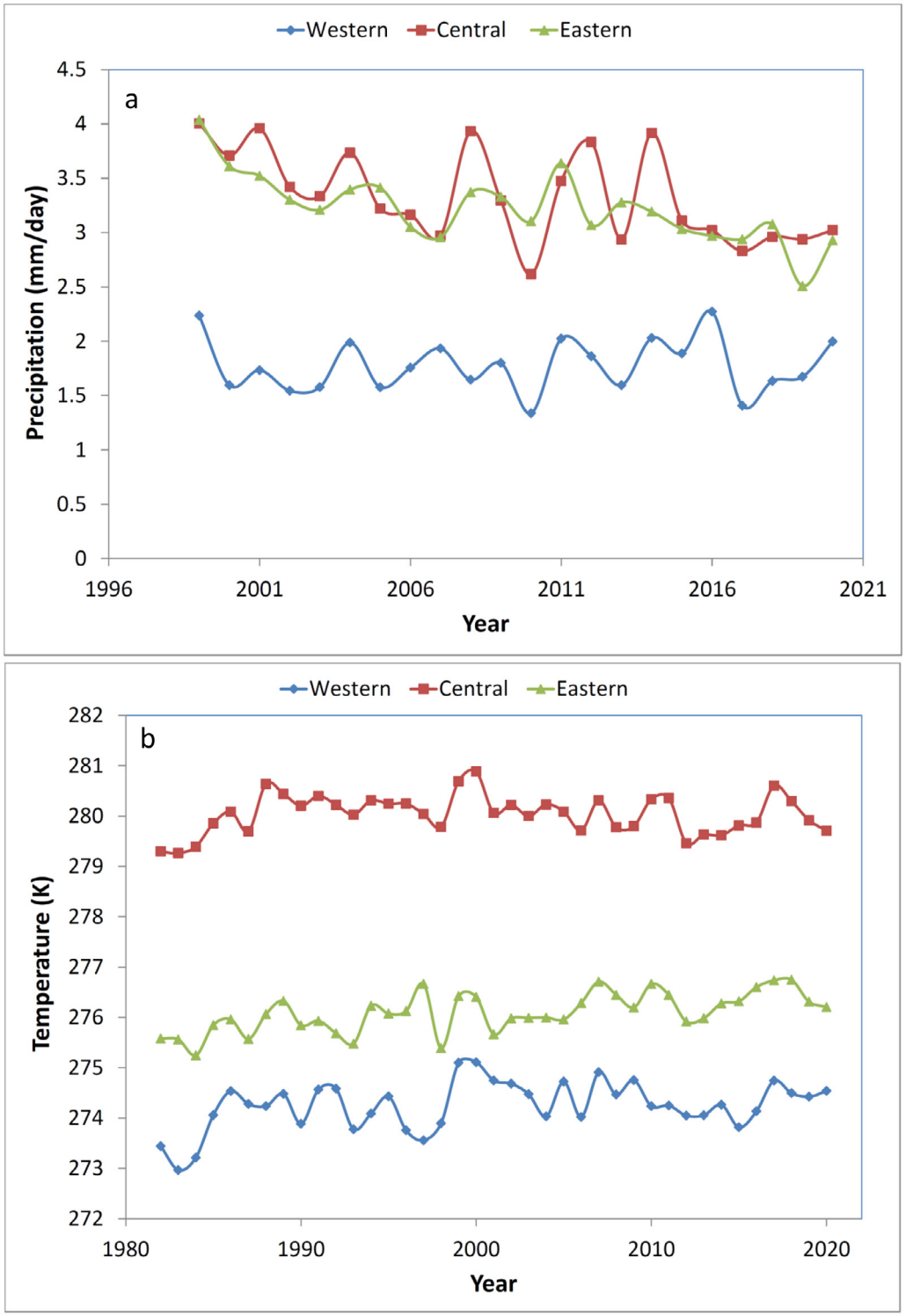

Fig. 5. Year-wise variation of precipitation (a) and skin temperature (b) along the Himalayan subdivision from 1984–2020.

H, I. Lake J also contains two subsidiary inputs: one from the mother glacier and another from a small lake present upstream. Lakes A, B, C and D coincide with avalanche and landslide-prone zones, marked here with brown boundary (Fig. 6). These lakes also experienced faster lake expansion by calving and waterline melting from the nearby glacier (Song et al., 2017). Thus, our detailed study marked A, B, C, F and I as critical. The semi-automatic method in previous sections exhibits the same. Xin et al. (2008) also showed Pida (B) and Longbasaba (A) lakes as GLOF-prone.

On the other hand, Lakes G, H and J are lesser prone to floods due to longer distances from avalanche-prone zones. Lakes D, G, H, J with medium GLOF probability are also of medium size, lesser increase rate and frontal width. Lastly, a minor Lake E shows the lowest GLOF probability.

Fieldwork was done in the Sikkim region at Gurudongmar Lake in 2015, dam overtopping was noticed, and the lake was half-frozen during fieldwork. In our result, this lake gives a lower GLOF probability. There is a lesser zone of GLOF as this lake contains two lower GLOF

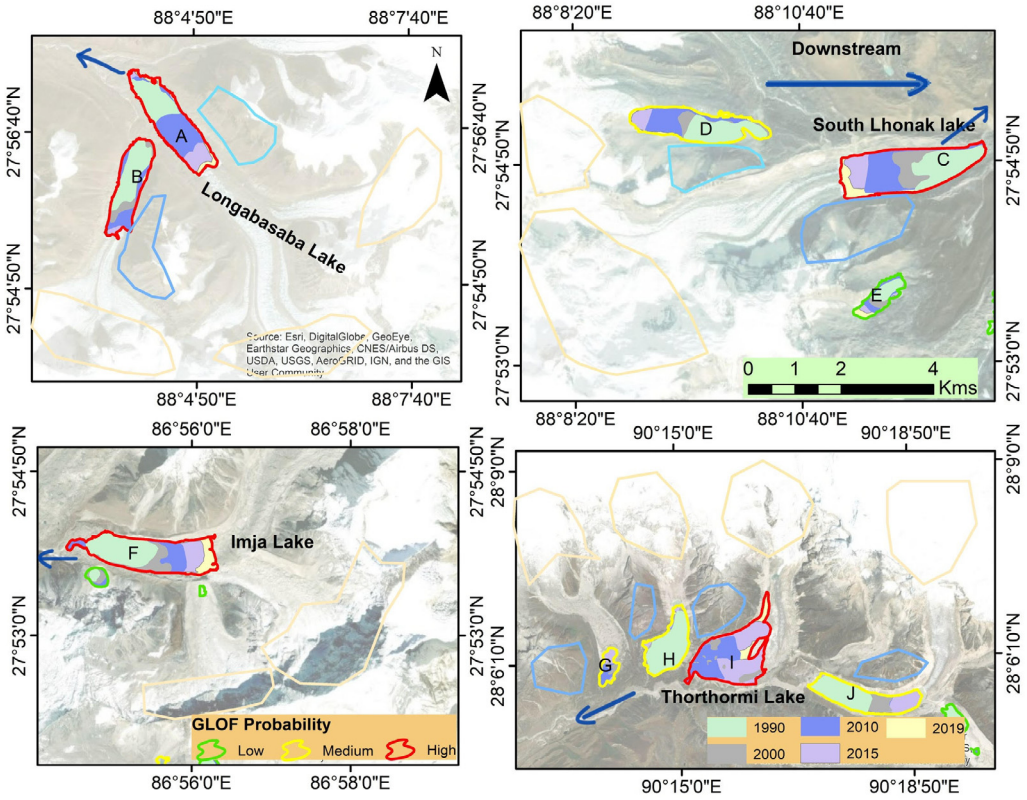

Fig. 6. Google Earth-based verification of selected glacial lakes (A, B, C, D and E of Sikkim; F in Nepal and G, H, I, and J of Bhutan Himalaya) and their derived GLOF probability. Here, A, B, C, D and E showing four glaciers within the Tista basin. Excluding lake E, all are high to medium GLOF-prone. Another high GLOF-prone lake F is the Imja in the Dudh Kosi river basin. Lake G, H, I, and J are present in Bhutan Himalaya's southern slope. Here, lake 'I' is higher prone to GLOF, and the rest are medium GLOF-prone lakes. The landslide and avalanches zone were highlighted in cyan and brown colour boundaries, respectively.

probable lakes with rock dammed on the upstream side (Fig. 7). These two upstream rock dammed lakes are more prone to avalanches and a very little chance of landslide. The lake's dam has not contained any dead ice; there is no local landslide chance, and hydraulic pressure on the dam is remaining constant due to the outlet's presence. However, with two rock dams on the upstream side, these two lakes are stable and less dangerous.

A good correlation was found between our results and previously published work by Aggarwal et al. (2017). A higher GLOF probability was determined for the Lhonak lake. Lake D in Fig. 6 gave a medium prone to GLOF in our and their result. Out of 21 glacial lakes, only 7 gave unmatched results in both the analysis. We got the odd consequence due to the different approaches and predictor parameters used in previous work and our methodology. In AHP methods, the weightage used here resembles previous works by Aggarwal et al. (2017). However, 13 lakes are closely matched in both the results. Besides, Gelhaipuco and Conqong lakes gave higher GLOF risk in the work of Che et al. (2014) (Fig. 8). Most of these higher GLOF prone lakes in our result are moraine-dammed lakes with a higher growth rate and present in the zone of higher earthquake-prone zones (Fig. 8).

5.5. GLOF probable zones basin wise in the Himalaya

Kosi river basin (33) contains the highest number of critical lakes, followed by Phelku and Tista (Table 3) (Fig. 9). Moreover, most GLOF prone lakes are gathered in the Langtang, Everest, Sikkim and Bhutan regions (eastern and central parts of the Himalaya). These regions contain the most populated areas of Himalaya, infrastructure with multiple roads and rail lines, and the second-highest hydroelectric plants (Schwanghart et al., 2016) (Fig. 9). Most of these dangerous lakes are connected to the southern flowing (27) drainage. The steeper drainage can accelerate the speed of floodwater. Moreover, the potential flood volume of water is more on the south than on the northern side of the Himalaya. Therefore, the southern sides of the Himalaya are more prone to GLOF than the northern side.

Glacial and topographical characteristics significantly control glacier ice area change on a local scale (Bhambri et al., 2011; Racoviteanu et al., 2014; Scherler et al., 2011). Previously, it was noticed that glaciers containing no lake have a lesser retreat rate than the glacier with lakes at its terminus (King et al., 2017; Racoviteanu et al., 2014; Bhambri et al., 2011). Most of the proglacial lakes are associated with clean glaciers of smaller size and mother glaciers with higher retreat rates (Mool et al., 2008; Bolch et al., 2012; King et al., 2017). These lakes are expanding significantly with waterline melting and calving processes. A higher area and length loss were estimated for clean glaciers, promoting proglacial lake formations (King et al., 2018; Garg et al., 2019). The southern side of the Himalaya contains a lake that has a higher increase rate (Komori, 2008; Debnath et al., 2018). A lesser lateral retreat rate was observed for higher debris content glaciers than lower debris content glaciers (clean glacier) due to the insulating effect of debris (King et al., 2018; Garg et al., 2019). The northern side glaciers showed the highest glacier area loss in recent decades, and most of the lakes associated with them are more likely to occur GLOF (24) (Nagai et al., 2013; Mohanty, 2018; King et al., 2018). Moreover, a southern side lake in this region contains higher debris-covered glaciers hence less retreat rate (Mohanty and Maiti, 2021). The southern side glaciers have more range elevation (relief) and potential debris supply slope, thus contain higher debris glaciers (Nagai et al., 2013; Ojha et al., 2017).

Wang et al. (2012) showed 142 glacial lakes prone to GLOF present in the Chinese Himalaya, using five controlling parameters. However, Wang et al. (2015) showed that the Chinese part of the Himalaya, i.e., the northern side of Sikkim, Bhutan, Langtang and Everest, are coming under a higher GLOF risk zone. Moreover, the Chinese part

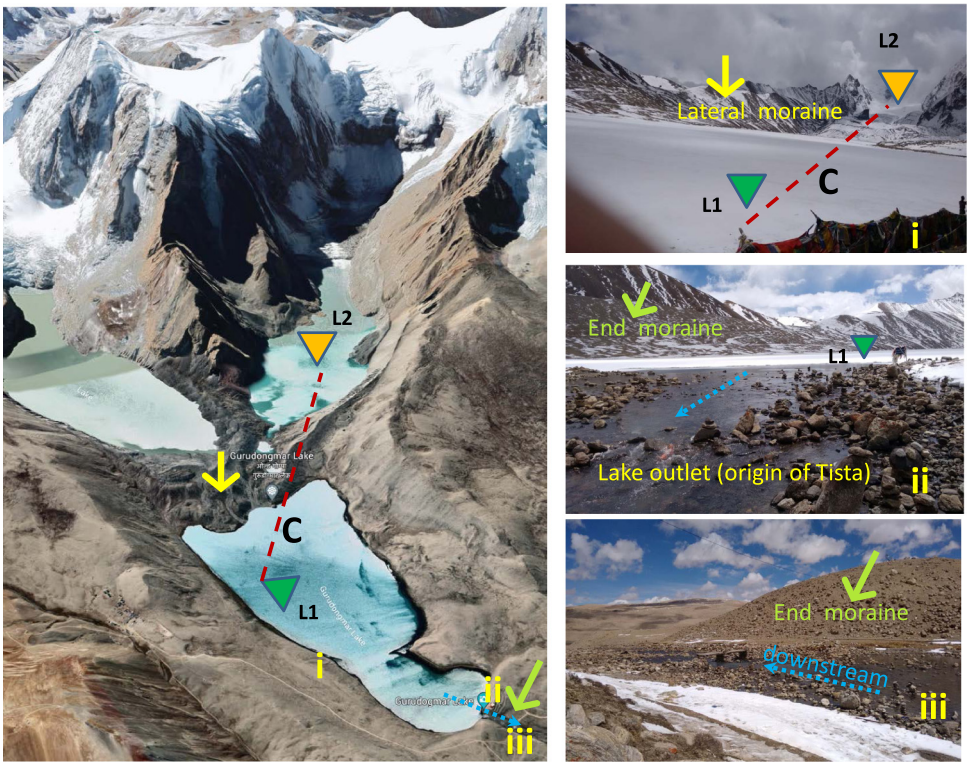

Fig. 7. Field visit in Gurudongmar Lake, North Sikkim. Field area and field photo locations from (i) to (iii), i.e. (i) frozen lake in higher altitude (L2) and Gurudongmar Lake (L1), (ii) Lake Outlet and origin of Tista river, (iv) Moraine dam. Green and yellow arrows indicate end and lateral moraine, respectively. In C elevation profile (L1 to L2) in Google Earth, all lakes cut across moraine in various elevation.

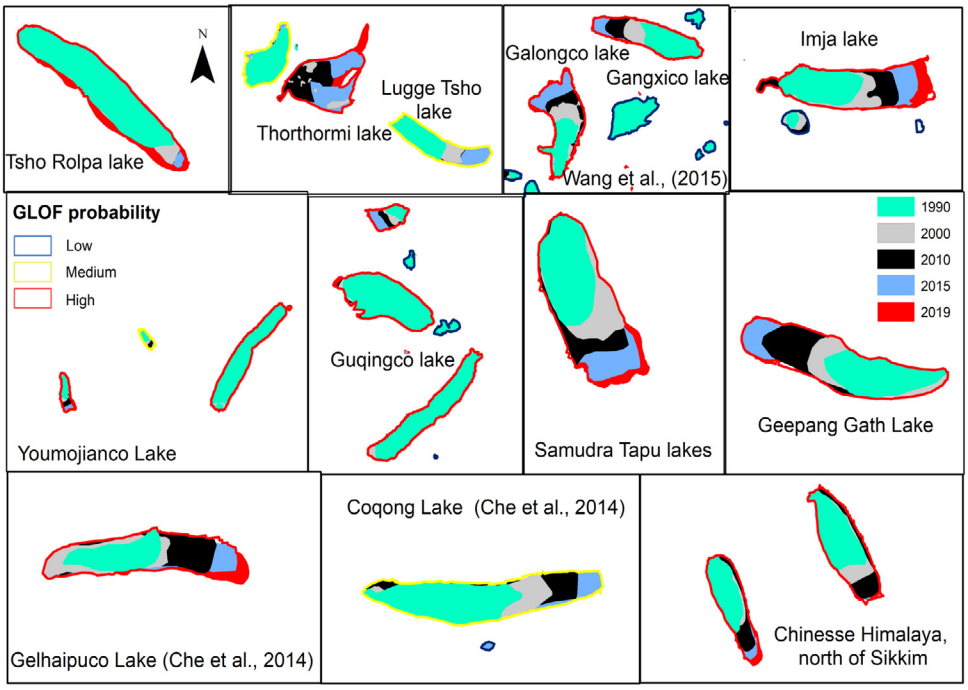

Fig. 8. Lake growth is shown for some selected higher prone GLOF lakes (Lake boundary red colour), medium (Lake boundary yellow colour), and lower (Lake boundary blue colour). Samudratapu and Geepang Gath lake are present in the western Himalaya, whereas all are central (Galongco, Guqingco, Imja, Tsho Rolpa, Youmojianco) or eastern Himalaya (Thorthormi).

of the Himalaya contains 116 GLOF prone lakes. However, this study categorizes the risk degree of the GLOF region wise and Nyalam, Tingri, Dinggye, and Lhozhang are in the very high-risk zone. Che et al. (2014) showed that most of the potential GLOF lakes are present in the Pumqu river basin and northern Sikkim and Nepal region, and their count is 19. Allen et al. (2019) showed Nyalam, Jilong, Dingri and Kangding as a higher risk zone of GLOF. Likewise, Worni et al. (2013) showed that the Sikkim region's glacial lakes gave higher GLOF risk, whereas

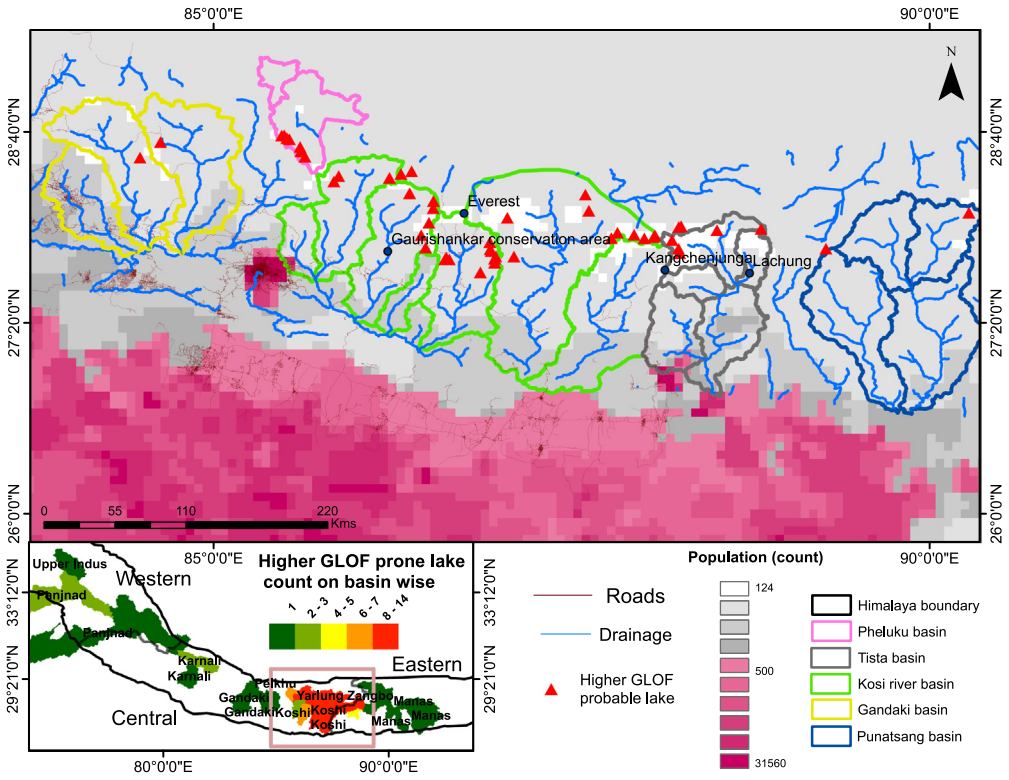

Fig. 9. GLOF probable zones demarcated in the Himalayas with their damage intensity. The basin wise critical lake count is shown for the whole Himalaya. Here green shows the lowest, and red shows the highest lake count. The raster layer shows the population counts in colour scale (red higher and cyan lower), whereas the red triangle indicates higher GLOF prone lakes. The blue dot shows some essential locations, and the brown line shows the road. Drainage and basin were exhibited in different colours.

lakes in Jammu and Kashmir and Uttarakhand gave lower GLOF risk. In contrast, Jammu and Kashmir region offers medium GLOF risk, precisely matching our result.

6. Conclusion

- A total of 60 glacial lakes were identified as high GLOF-prone lakes in the Himalaya. These lakes are primarily located in Central Himalaya (46), followed by Eastern (10) and Western Himalaya (4). Sub-regionally, most of them are in Sikkim, Everest, Langtang and Bhutan regions. Kosi (33) river basin contains the highest number of critical lakes, followed by Phelku (7) and Tista (5). Coincidentally, most GLOF-prone lakes are connected to the southernly flowing streams.
- 164 and 3974 numbers of lakes were identified as medium and lower prone to GLOF. The medium GLOF-prone and glacial connected lakes will increase in size at a higher rate by calving and waterline melting process; hence dangerous.
- Identified high GLOF-prone lakes should be studied in details with field estimation of peak discharge, overtopping duration and flood route identification for sustainable development and mitigations.

Declaration of competing interest

The authors declare that they have no known competing financial interests or personal relationships that could have appeared to influence the work reported in this paper.

Acknowledgements

The work is partially financed by ISIRD and Institute CPDA grants of IIT Kharagpur. We collected satellite images from USGS and the database from ICIMOD. We want to thank Dr. Manik Das Adhikari, Anup Bera and Benudhar Pradhan for their help during the geodatabase creation.

References

Aggarwal, S., Rai, S.C., Thakur, P.K., Emmer, A., 2017. Inventory and recently increasing GLOF susceptibility of glacial lakes in Sikkim, Eastern Himalaya. Geomorphology 295, 39–54.

Alcántara-Ayala, I., 2002. Geomorphology, natural hazards, vulnerability and prevention of natural disasters in developing countries. Geomorphology 47 (2–4), 107–124.

Alean, J., 1985. Ice avalanches: some empirical information about their formation and reach. J. Glaciol. 31 (109), 324–333.

Allen, S.K., Linsbauer, A., Randhawa, S.S., Huggel, C., Rana, P., Kumari, A., 2016. Glacial lake outburst flood risk in Himachal Pradesh, India: an integrative and anticipatory approach considering current and future threats. Nat. Hazards 84 (3), 1741–1763.

Allen, S.K., Zhang, G., Wang, W., Yao, T., Bolch, T., 2019. Potentially dangerous glacial lakes across the Tibetan Plateau revealed using a large-scale automated assessment approach. Sci. Bull. 64 (7), 435–445.

Ayalew, L., Yamagishi, H., Marui, H., Kanno, T., 2005. Landslides in Sado Island of Japan: Part II. GIS-based susceptibility mapping with comparisons of results from two methods and verifications. Eng. Geol. 81 (4), 432–445.

Bajracharya, S.R., Maharjan, S.B., Shrestha, F., 2014. The status and decadal change of glaciers in Bhutan from the 1980s to 2010 based on satellite data. Ann. Glaciol. 55 (66), 159–166.

Bajracharya, S.R., Mool, P., 2009. Glaciers, glacial lakes and glacial lake outburst floods in the Mount Everest region, Nepal. Ann. Glaciol. 50 (53), 81–86.

Bajracharya, S.R., Mool, P.K., Shrestha, B.R., 2008a. Global climate change and melting of Himalayan glaciers. In: Melting Glaciers and Rising Sea Levels: Impacts and Implications. pp. 28–46.

Bajracharya, S.R., Mool, P.K., Shrestha, B.R., 2008b. Mapping of glacial lakes and GLOF in the Himalayas. In: Policy Priorities for Sustainable Mountain Development. Full Proceedings of the ICIMOD Regional Policy Workshop, Kathmandu, Nepal, 18-20 September, 2006. International Centre for Integrated Mountain Development (ICIMOD).

Bathrellos, G.D., Gaki-Papanastassiou, K., Skilodimou, H.D., Papanastassiou, D., Chousianitis, K.G., 2012. Potential suitability for urban planning and industry development using natural hazard maps and geological–geomorphological parameters. Environ. Earth Sci. 66 (2), 537–548.

Bhambri, R., Bolch, T., Chaujar, R.K., Kulshreshtha, S.C., 2011. Glacier changes in the Garhwal Himalaya, India, from 1968 to 2006 based on remote sensing. J. Glaciol. 57 (203), 543–556.

Bolch, T., Kulkarni, A., Kääb, A., Huggel, C., Paul, F., Cogley, J.G., et al., 2012. The state and fate of Himalayan glaciers. Science 336 (6079), 310–314.

Bookhagen, B., Burbank, D.W., 2010. Toward a complete Himalayan hydrological budget: Spatiotemporal distribution of snowmelt and rainfall and their impact on river discharge. J. Geophys. Res. Earth Surf. 115 (F3).

Brown, M.E., Racoviteanu, A.E., Tarboton, D.G., Gupta, A.S., Nigro, J., Policelli, F., et al., 2014. An integrated modeling system for estimating glacier and snow melt driven streamflow from remote sensing and earth system data products in the himalayas. J. Hydrol. 519, 1859–1869.

Brun, F., Wagnon, P., Berthier, E., Jomelli, V., Maharjan, S.B., Shrestha, F., Kraaijenbrink, P.D.A., 2019. Heterogeneous influence of glacier morphology on the mass balance variability in High Mountain Asia. J. Geophys. Res. Earth Surf. 124 (6), 1331–1345.

Carrivick, J.L., Tweed, F.S., 2016. A global assessment of the societal impacts of glacier outburst floods. Glob. Planet. Change 144, 1–16.

Che, T., Xiao, L., Liou, Y.A., 2014. Changes in glaciers and glacial lakes and the identification of dangerous glacial lakes in the Pumqu River Basin, Xizang (Tibet). Adv. Meteorol. 2014.

Chen, F.H., Bloemendal, J., Zhang, P.Z., Liu, G.X., 1999. An 800 ky proxy record of climate from lake sediments of the Zoige Basin, eastern Tibetan Plateau. Palaeogeogr. Palaeoclimatol. Palaeoecol. 151 (4), 307–320.

Chiarle, M., Iannotti, S., Mortara, G., Deline, P., 2007. Recent debris flow occurrences associated with glaciers in the Alps. Glob. Planet. Change 56 (1–2), 123–136.

Clague, J.J., Evans, S.C., 2000. A review of catastrophic drainage of moraine-dammed lakes in British Columbia. Quat. Sci. Rev. 19 (17–18), 1763–1783.

Costa, J.E., Schuster, R.L., 1988. The formation and failure of natural dams. Geol. Soc. Am. Bull. 100 (7), 1054–1068.

Das, S., Kar, N.S., Bandyopadhyay, S., 2015. Glacial lake outburst flood at Kedarnath, Indian Himalaya: a study using digital elevation models and satellite images. Nat. Hazards 77 (2), 769–786.

Debnath, M., Syiemlieh, H.J., Sharma, M.C., Kumar, R., Chowdhury, A., Lal, U., 2018. Glacial lake dynamics and lake surface temperature assessment along the Kangchengayo-Pauhunri Massif, Sikkim Himalaya, 1988–2014. Remote Sens. Appl.: Soc. Environ. 9, 26–41.

Deline, P., Gruber, S., Delaloye, R., Fischer, L., Geertsema, M., Giardino, M., et al., 2015. Ice loss and slope stability in high-mountain regions. In: Snow and Ice-Related Hazards, Risks and Disasters. Academic Press, pp. 521–561.

Ding, M., Gao, Z., Huang, T., Hu, X., 2020. The hazard assessment of glacial lake debris flow: A case study on dongcuoqu, luolong county, tibet. In: IOP Conference Series: Earth and Environmental Science, Vol. 570, (4). IOP Publishing, 042054.

Duan, Y., Liu, T., Meng, F., Yuan, Y., Luo, M., Huang, Y., et al., 2020. Accurate simulation of ice and snow runoff for the mountainous terrain of the kunlun mountains, China. Remote Sens. 12 (1), 179.

Dufresne, A., Wolken, G.J., Hibert, C., Bessette-Kirton, E.K., Coe, J.A., Geertsema, M., Ekström, G., 2019. The 2016 Lamplugh rock avalanche, Alaska: deposit structures and emplacement dynamics. LandSlides 16 (12), 2301–2319.

Emmer, A., Klimeˇ s, J., Mergili, M., Vilímek, V., Cochachin, A., 2016. 882 lakes of the Cordillera Blanca: an inventory, classification, evolution and assessment of susceptibility to outburst floods. Catena 147, 269–279.

Falaschi, D., Kääb, A., Paul, F., Tadono, T., Rivera, J.A., Lenzano, L.E., 2019. Brief communication: Collapse of 4 Mm 3 of ice from a cirque glacier in the Central Andes of Argentina. Cryosphere 13 (3), 997–1004.

Farinotti, D., Huss, M., Fürst, J.J., Landmann, J., Machguth, H., Maussion, F., Pandit, A., 2019. A consensus estimate for the ice thickness distribution of all glaciers on Earth. Nat. Geosci. 12 (3), 168–173.

Feldmann, J., Levermann, A., 2015. Collapse of the West Antarctic Ice Sheet after local destabilization of the Amundsen Basin. Proc. Natl. Acad. Sci. 112 (46), 14191–14196.

Frey, H., Haeberli, W., Linsbauer, A., Huggel, C., Paul, F., 2010. A multi-level strategy for anticipating future glacier lake formation and associated hazard potentials. Nat. Hazards Earth Syst. Sci. 10 (2), 339–352.

Fujita, K., Sakai, A., Nuimura, T., Yamaguchi, S., Sharma, R.R., 2009. Recent changes in Imja Glacial Lake and its damming moraine in the Nepal Himalaya revealed by in situ surveys and multi-temporal ASTER imagery. Environ. Res. Lett. 4 (4), 045205.

Fujita, K., Sakai, A., Takenaka, S., Nuimura, T., Surazakov, A.B., Sawagaki, T., Yamanokuchi, T., 2013. Potential flood volume of Himalayan glacial lakes. Nat. Hazards Earth Syst. Sci. 13 (7), 1827–1839.

Gardelle, J., Arnaud, Y., Berthier, E., 2011. Contrasted evolution of glacial lakes along the Hindu Kush Himalaya mountain range between 1990 and 2009. Glob. Planet. Change 75 (1–2), 47–55.

Gardelle, J., Berthier, E., Arnaud, Y., Kääb, A., 2013. Region-wide glacier mass balances over the Pamir-Karakoram-Himalaya during 1999-2011. Cryosphere 7 (6), 1263.

Garg, P.K., Shukla, A., Jasrotia, A.S., 2019. On the strongly imbalanced state of glaciers in the Sikkim, eastern Himalaya, India. Sci. Total Environ. 691, 16–35.

Ghosh, S., Pandey, A.C., Nathawat, M.S., Bahuguna, I.M., 2014. Contrasting signals of glacier changes in Zanskar valley, Jammu & Kashmir, India using remote sensing and GIS. J. Indian Soc. Remote Sens. 42 (4), 817–827.

Goswami, U.P., Goyal, M.K., 2021. Assessment of glacial lake development and downstream flood impacts of critical glacial lake. Nat. Hazards 1–20.

Harrison, S., Glasser, N., Winchester, V., Haresign, E., Warren, C., Jansson, K., 2006. A glacial lake outburst flood associated with recent mountain glacier retreat, Patagonian Andes. Holocene 16 (4), 611–620.

Harrison, S., Kargel, J.S., Huggel, C., Reynolds, J., Shugar, D.H., Betts, R.A., et al., 2018. Climate change and the global pattern of moraine-dammed glacial lake outburst floods. Cryosphere 12 (4), 1195–1209.

Hartmann, J., Moosdorf, N., 2012. The new global lithological map database GLiM: A representation of rock properties at the Earth surface. Geochem. Geophys. Geosystems 13 (12).

Hogg, A.E., Gudmundsson, G.H., 2017. Impacts of the Larsen-C Ice Shelf calving event. Nature Clim. Change 7 (8), 540–542.

Hosseinali, F., Alesheikh, A.A., 2008. Weighting spatial information in GIS for copper mining exploration. Am. J. Appl. Sci. 5 (9), 1187–1198.

Hubbard, A., Hein, A.S., Kaplan, M.R., Hulton, N.R., Glasser, N., 2005. A modelling reconstruction of the last glacial maximum ice sheet and its deglaciation in the vicinity of the Northern Patagonian Icefield, South America. Geografiska Ann.: Ser. A Phys. Geogr. 87 (2), 375–391.

Huggel, C., 2004. Assessment of glacial hazards based on remote sensing and gis modeling. Department of Geography, University of Zurich, Phys. Geogr. Ser. 44 (2004).

Huggel, C., Kääb, A., Haeberli, W., Teysseire, P., Paul, F., 2002. Remote sensing based assessment of hazards from glacier lake outbursts: a case study in the Swiss Alps. Can. Geotech. J. 39 (2), 316–330.

ICIMOD, 2011. ICIMOD Glacial Lakes and Glacial Lake Outburst Floods in Nepal. ICIMOD, Kathmandu, Nepal.

Iribarren Anacona, P., Norton, K.P., Mackintosh, A., 2014. Moraine-dammed lake failures in Patagonia and assessment of outburst susceptibility in the Baker Basin. Nat. Hazards Earth Syst. Sci. 14 (12), 3243–3259.

Joughin, I., Smith, B.E., Medley, B., 2014. Marine ice sheet collapse potentially under way for the Thwaites Glacier Basin, West Antarctica. Science 344 (6185), 735–738.

Kääb, A., Berthier, E., Nuth, C., Gardelle, J., Arnaud, Y., 2012. Contrasting patterns of early twenty-first-century glacier mass change in the Himalayas. Nature 488 (7412), 495–498.

Kääb, A., Leinss, S., Gilbert, A., Bühler, Y., Gascoin, S., Evans, S.G., et al., 2018. Massive collapse of two glaciers in western Tibet in 2016 after surge-like instability. Nat. Geosci. 11 (2), 114–120.

Kääb, A., Reichmuth, T., 2005. Advance mechanisms of rockglaciers. Permafr. Periglac. Process. 16 (2), 187–193.

Kanamitsu, M., Kumar, A., Juang, H.M.H., Schemm, J.K., Wang, W., Yang, F., et al., 2002. NCEP dynamical seasonal forecast system 2000. Bull. Am. Meteorol. Soc. 83 (7), 1019–1038.

Kargel, J.S., Abrams, M.J., Bishop, M.P., Bush, A., Hamilton, G., Jiskoot, H., et al., 2005. Multispectral imaging contributions to global land ice measurements from space. Remote Sens. Environ. 99 (1–2), 187–219.

Kargel, J.S., Leonard, G.J., Shugar, D.H., Haritashya, U.K., Bevington, A., Fielding, E.J., et al., 2016. Geomorphic and geologic controls of geohazards induced by Nepal's 2015 Gorkha earthquake. Science 351 (6269), aac8353.

Kayastha, P., Dhital, M.R., De Smedt, F., 2013. Application of the analytical hierarchy process (AHP) for landslide susceptibility mapping: a case study from the Tinau watershed, west Nepal. Comput. Geosci. 52, 398–408.

Keefer, D.K., 1984. Landslides caused by earthquakes. Geol. Soc. Am. Bull. 95 (4), 406–421.

Keefer, D.K., 2002. Investigating landslides caused by earthquakes–a historical review. Surv. Geophys. 23 (6), 473–510.

King, O., Dehecq, A., Quincey, D., Carrivick, J., 2018. Contrasting geometric and dynamic evolution of lake and land-terminating glaciers in the central Himalaya. Glob. Planet. Change 167, 46–60.

King, O., Quincey, D.J., Carrivick, J.L., Rowan, A.V., 2017. Spatial variability in mass loss of glaciers in the Everest region, central Himalayas, between 2000 and 2015. Cryosphere.

Komori, J., 2008. Recent expansions of glacial lakes in the Bhutan Himalayas. Quat. Int. 184 (1), 177–186.

Kulkarni, A.V., Bahuguna, I.M., Rathore, B.P., Singh, S.K., Randhawa, S.S., Sood, R.K., Dhar, S., 2007. Glacial retreat in Himalaya using Indian remote sensing satellite data. Current Sci. 6, 9–74.

Kumar, S., Srivastava, P.K., Snehmani, 2017. GIS-based MCDA–AHP modelling for avalanche susceptibility mapping of Nubra valley region, Indian Himalaya. Geocarto Int. 32 (11), 1254–1267.

Lari, S., Frattini, P., Crosta, G.B., 2009. Integration of natural and technological risks in Lombardy, Italy. Nat. Hazards Earth Syst. Sci. 9 (6), 2085–2106.

Li, C., Yan, F., Kang, S., Yan, C., Hu, Z., Chen, P., et al., 2021. Carbonaceous matter in the atmosphere and glaciers of the Himalayas and the Tibetan plateau: An investigative review. Environ. Int. 146, 106281.

Liu, J.J., Cheng, Z.L., Su, P.C., 2014. The relationship between air temperature fluctuation and Glacial Lake Outburst Floods in Tibet, China. Quat. Int. 321, 78–87.
Lliboutry, L., Arnao, B.M., Pautre, A., Schneider, B., 1977. Glaciological problems set by the control of dangerous lakes in Cordillera Blanca, Peru. I. Historical failures of morainic dams, their causes and prevention. J. Glaciol. 18 (79), 239–254.
Lu, R., Tang, B., Li, D., 1999. Introduction of debris flow resulted from glacial lakes failed. Debris Flow and Environment in Tibet, Chengdu (China), pp. 69–105.
MacLean, M.G., Congalton, R.G., 2012, March. Map accuracy assessment issues when using an object-oriented approach. In: Proceedings of the American Society for Photogrammetry and Remote Sensing 2012 Annual Conference, Sacramento, CA, USA, pp. 19–23.
Marana, B., 2017. An ArcGIS geo-morphological approach for snow avalanche zoning and risk estimation in the Province of Bergamo.
Mayewski, P.A., Jeschke, P.A., 1979. Himalayan and Trans-Himalayan glacier fluctuations since AD 1812. Arct. Alp. Res. 11 (3), 267–287.
McKillop, R.J., Clague, J.J., 2007. Statistical, remote sensing-based approach for estimating the probability of catastrophic drainage from Moraine-Dammed Lakes in Southwestern British Columbia. Glob. Planet. Change 56 (1–2), 153–171.
Meena, S.R., Bhuyan, K., Chauhan, A., Singh, R.P., 2021. Snow covered with dust after Chamoli rockslide: inference based on high-resolution satellite data. Remote Sens. Lett. 12 (7), 704–714.
Mohanty, L., 2018, April. Spatio-temporal glacier area change analysis in the Himalayan: A comparison between northerly and southerly flowing glaciers. In: EGU General Assembly Conference Abstracts, p. 19280.
Mohanty, L.K., Maiti, S., 2021. Regional morphodynamics of supraglacial lakes in the Everest Himalaya. Sci. Total Environ. 751, 141586.
Mool, P.K., Wangda, D., Bajracharya, S.R., Karma, D.R., Joshi, S.P., 2001. Inventory of Glaciers, Glacial Lakes and Glacial Lake Outburst Floods, Bhutan. ICIMOD, Kathmandu, p. 247.
Nagai, H., Fujita, K., Nuimura, T., Sakai, A., 2013. Southwest-facing slopes control the formation of debris-covered glaciers in the Bhutan Himalaya. Cryosphere 7 (4), 1303.
Nath, S.K., 2004. Seismic hazard mapping and microzonation in the Sikkim Himalaya through GIS integration of site effects and strong ground motion attributes. Nat. Hazards 31, 319–342.
Nie, Y., Liu, Q., Wang, J., Zhang, Y., Sheng, Y., Liu, S., 2018. An inventory of historical glacial lake outburst floods in the Himalayas based on remote sensing observations and geomorphological analysis. Geomorphology 308, 91–106.
Nie, Y., Sheng, Y., Liu, Q., Liu, L., Liu, S., Zhang, Y., Song, C., 2017. A regional-scale assessment of himalayan glacial lake changes using satellite observations from 1990 to 2015. Remote Sens. Environ. 189, 1–13.
O'Connor, J.E., Hardison, J.H., Costa, J.E., 2001. Debris flows from failures of neoglacial-age moraine dams in the Three Sisters and Mount Jefferson Wilderness Areas. Geological Survey, Reston, Virginia, Oregon, US.
Ojha, S., Fujita, K., Sakai, A., Nagai, H., Lamsal, D., 2017. Topographic controls on the debris- cover extent of glaciers in the Eastern Himalayas: Regional analysis using a novel high- resolution glacier inventory. Quat. Int. 455, 82–92.
Peduzzi, P., 2010. Landslides and vegetation cover in the 2005 North Pakistan earthquake: a GIS and statistical quantitative approach. Nat. Hazards Earth Syst. Sci. 10 (4), 623–640.
Racoviteanu, A., Arnaud, Y., Williams, M.W., Manley, W.F., 2014. Spatial patterns in glacier characteristics and area changes from 1962 to 2006 in the Kanchenjunga–Sikkim area, eastern Himalaya. Cryosphere 9, 505–523.
Richardson, S.D., Reynolds, J.M., 2000. An overview of glacial hazards in the Himalayas.
Saaty, T.L., 1987. Rank generation, preservation, and reversal in the analytic hierarchy decision process. Decis. Sci. 18 (2), 157–177.
Sattar, A., Goswami, A., Kulkarni, A.V., 2019. Application of 1D and 2D hydrodynamic modeling to study glacial lake outburst flood (GLOF) and its impact on a hydropower station in Central Himalaya. Nat. Hazards 97 (2), 535–553.
Sattar, A., Goswami, A., Kulkarni, A., Emmer, A., 2020. Lake evolution, hydrodynamic outburst flood modeling and sensitivity analysis in the Central Himalaya: a case study. Water 12 (1), 237.
Scherler, D., Bookhagen, B., Strecker, M.R., 2011. The spatially variable response of Himalayan glaciers to climate change affected by debris cover. Nat. Geosci. 4 (3), 156–159.
Schwanghart, W., Worni, R., Huggel, C., Stoffel, M., Korup, O., 2016. Uncertainty in the Himalayan energy–water nexus: Estimating regional exposure to glacial lake outburst floods. Environ. Res. Lett. 11 (7), 074005.
Song, C.Q., Sheng, Y.W., Wang, J.D., Ke, L.H., Madson, A., Nie, Y., 2017. Heterogeneous glacial lake changes and links of lake expansions to the rapid thinning of adjacent glacier termini in the Himalayas. Geomorphology 280, 30–38.
Veh, G., Korup, O., von Specht, S., Roessner, S., Walz, A., 2019. Unchanged frequency of moraine-dammed glacial lake outburst floods in the Himalaya. Nature Clim. Change 9 (5), 379–383.
Walder, J.S., Watts, P., Sorensen, O.E., Janssen, K., 2003. Tsunamis generated by subaerial mass flows. J. Geophys. Res. Solid Earth 108 (B5).
Wang, X., Liu, Q.H., Liu, S.Y., Wei, J.F., Jiang, Z.L., 2016. Heterogeneity of glacial lake expansion and its contrasting signals with climate change in Tarim Basin, Central Asia. Environ. Earth Sci. 75, 696.
Wang, W., Yang, X., Yao, T., 2012. Evaluation of ASTER GDEM and SRTM and their suitability in hydraulic modelling of a glacial lake outburst flood in southeast Tibet. Hydrol. Process. 26 (2), 213–225.
Wang, W., Yao, T., Gao, Y., Yang, X., Kattel, D.B., 2011. A first-order method to identify potentially dangerous glacial lakes in a region of the southeastern Tibetan Plateau. Mt. Res. Dev. 31 (2), 122–130.
Wilson, R., Harrison, S., Reynolds, J., Hubbard, A., Glasser, N.F., Wündrich, O., Iribarren Anacona, P., Mao, L., Shannon, S., 2015. Chileno Valley glacial lake outburst flood, Patagonia. Geomorphology 332 (2019), 51–65.
Worni, R., Huggel, C., Stoffel, M., 2013. Glacial lakes in the Indian Himalayas—From an area- wide glacial lake inventory to on-site and modeling based risk assessment of critical glacial lakes. Sci. Total Environ. 468, S71–S84.
Xin, W., Shiyin, L., Wanqin, G., Junli, X., 2008. Assessment and simulation of glacier lake outburst floods for Longbasaba and Pida Lakes, China. Mt. Res. Dev. 28 (3), 310–317.
Yao, T., Thompson, L., Yang, W., Yu, W., Gao, Y., Guo, X., et al., 2012. Different glacier status with atmospheric circulations in Tibetan Plateau and surroundings. Nature Clim. Change 2 (9), 663–667.
Zaidi, A.Z., Yasmeen, Z., Siddiqui, M.D., 2013. Glacial lake outburst flood (GLOF) Risk mapping in Hunza River Basin (Pakistan) using geospatial techniques. In: 2013 6th International Conference on Recent Advances in Space Technologies (RAST). IEEE, pp. 191–195.
Zhang, G., Yao, T., Xie, H., Wang, W., Yang, W., 2015. An inventory of glacial lakes in the Third Pole region and their changes in response to global warming. Glob. Planet. Change 131, 148–157.
Zheng, G., Bao, A., Allen, S., Ballesteros-Cánovas, J., Yuan, Y., Jiapaer, G., Stoffel, M., 2021. Numerous unreported glacial lake outburst floods in the Third Pole revealed by high-resolution satellite data and geomorphological evidence. Sci. Bull..